SUPPORTING INFORMATION

Inverted Si:PbS Colloidal Quantum Dots Heterojunction Based Infrared Photodetector

Kaimin Xu,[a‡] *Xiongbin Xiao,*[a,c,d‡] *Wenjia Zhou,*[a] *Xianyuan Jiang,*[a] *Qi Wei,*[a] *Hao Chen,*[a] *Zhuo Deng,*[b] *Jian Huang,*[b] *Baile Chen,*[b] *Zhijun Ning*[a]*

[a] School of Physical Science and Technology, ShanghaiTech University, 393 Middle Huaxia Road, Pudong, Shanghai, 201210, China

[b] School of Information Science and Technology, ShanghaiTech University, 393 Middle Huaxia Road, Pudong, Shanghai, 201210, China

[c] State Key Laboratory of Functional Materials for Informatics, Shanghai Institute of Microsystem and Information Technology, Chinese Academy of Sciences, Shanghai 200050, China

[d] University of Chinese Academy of Sciences, Beijing 100049, China

‡ Equal contribution.
* Corresponding author (E-mail: ningzhj@shanghaitech.edu.cn).

Chemicals

Lead Oxide (PbO, Aladdin, 99.99%), Oleic Acid (OA, Aladdin, AR), Oleylamine (OLA, Aladdin, 80-90%), Octadecene (ODE, Aladdin, 90%), Hexamethyldisilathiane ($(TMS)_2S$, Aldrich, synthesis grade), Iodine (I_2, Aladdin, 99.8%), Cadmium Chloride (CdCl2, Aladdin, 99.99%), N-tetradecylphosphonic acid (TDPA, Energy Chemical, 98%), Acetone (Sinopharm, AR), Octane (Aladdin, AR, 96%), 1,2-Ethanedithiol (EDT, Sigma-Aldrich, 98%), Acetonitrile (Aladdin, 95%), Silicon wafer (n(100) 0.01-0.02 Ω.cm, 2-4 Ω.cm, 10-20 Ω.cm, Suzhou Crystal Silicon electronic & Technology Co., Ltd).

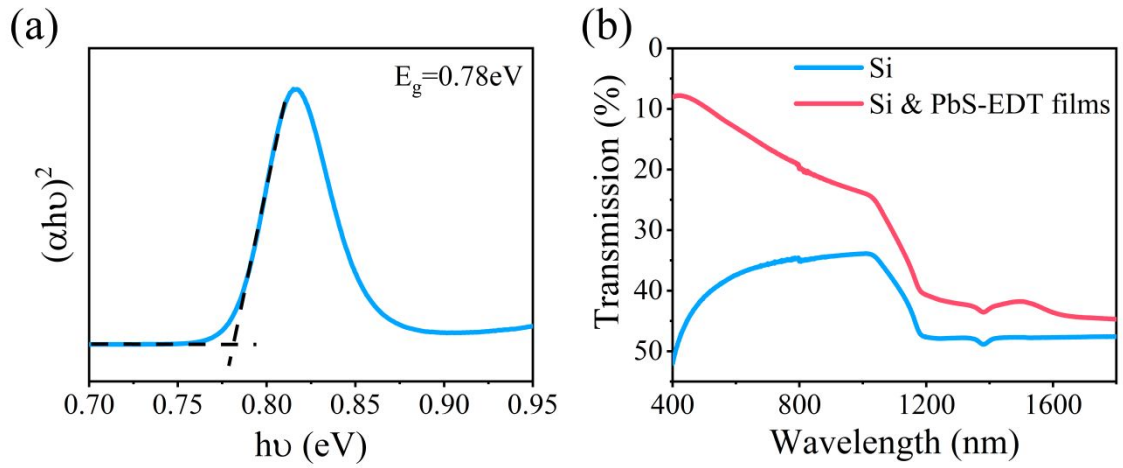

Figure S1. (a) Tauc plot of PbS CQDs calculated from the absorption spectrum. The bandgap of PbS CQDs in this work was 0.78 eV. (b) Transmission spectra of Si wafer and the Si wafer with PbS-EDT layer. The usage of PbS-EDT layer entends the photosensity range of Si wafer.

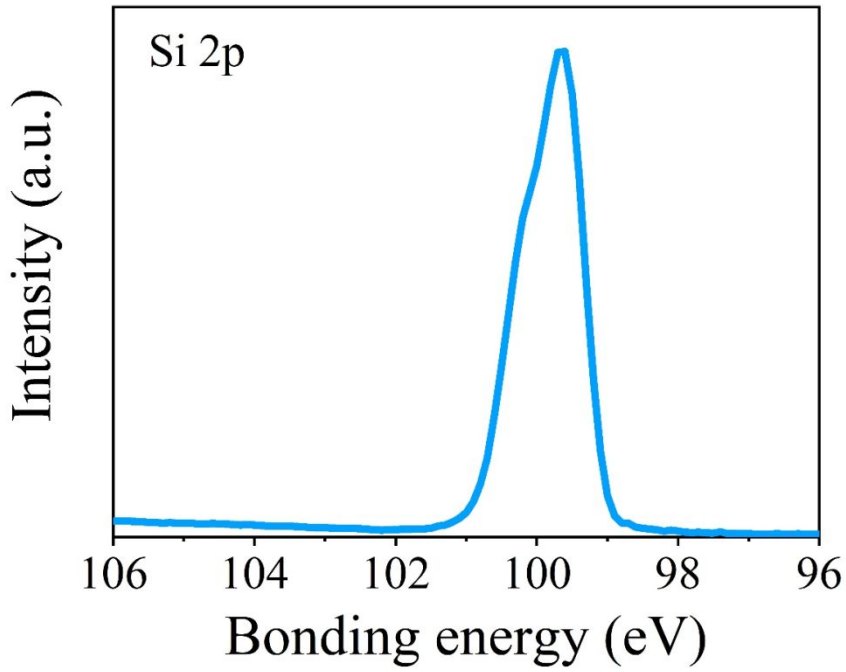

Figure S2. XPS spectrum of Si wafer after RCA cleaning process. There is not SiOx signal existing that confirms the elimination of SiO_x on Si wafer's surface.

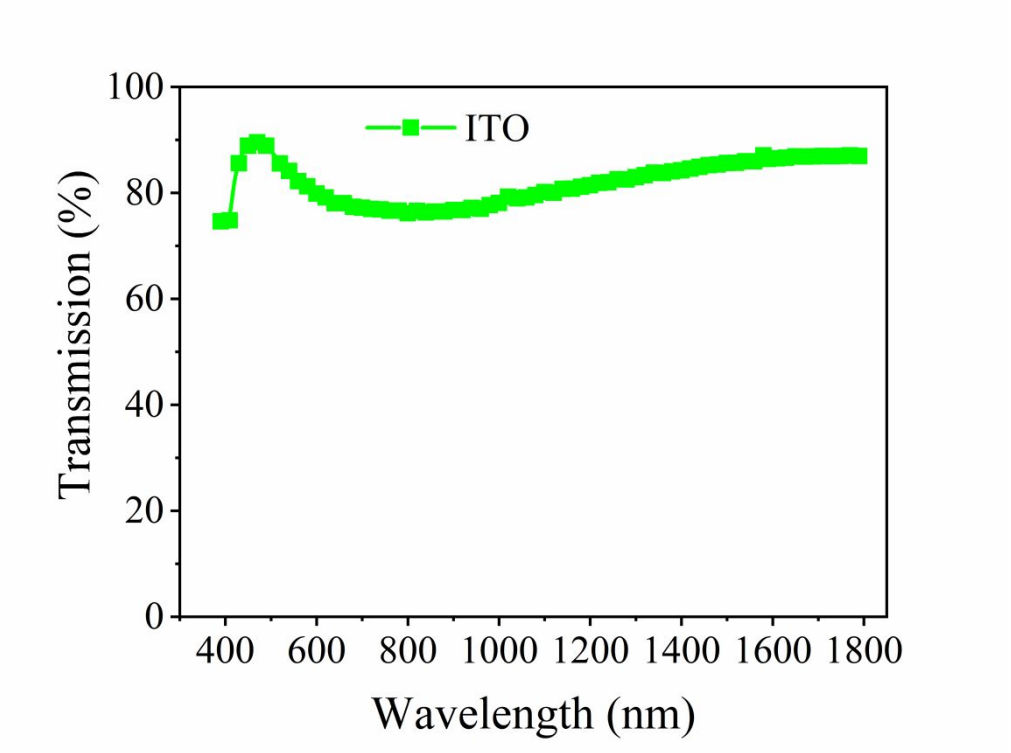

Figure S3. Transparent spectrum of ITO.

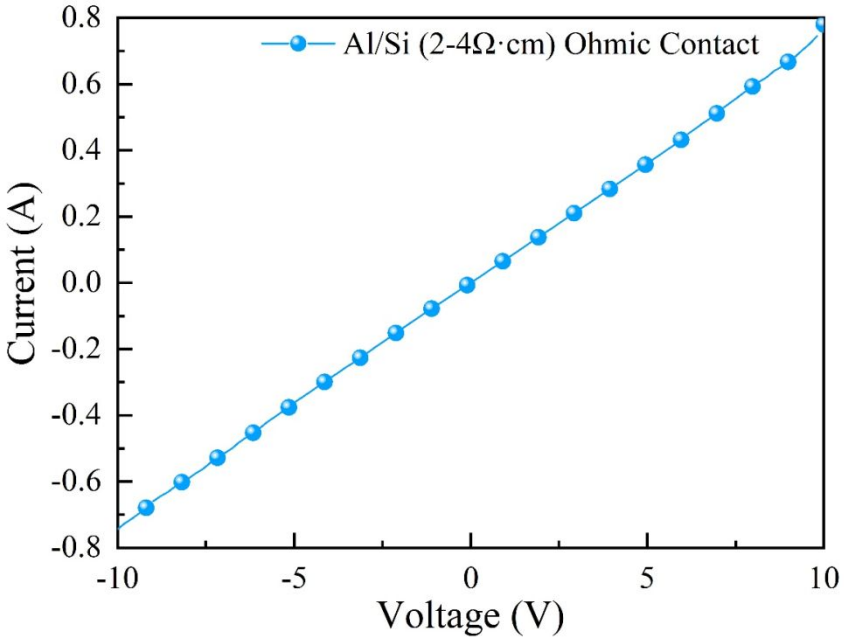

Figure S4. IV curve of Al/Si/Al structure device. Symmetrical and stright line of IV curve indicates that the Al and Si wafer is Ohmic contact.

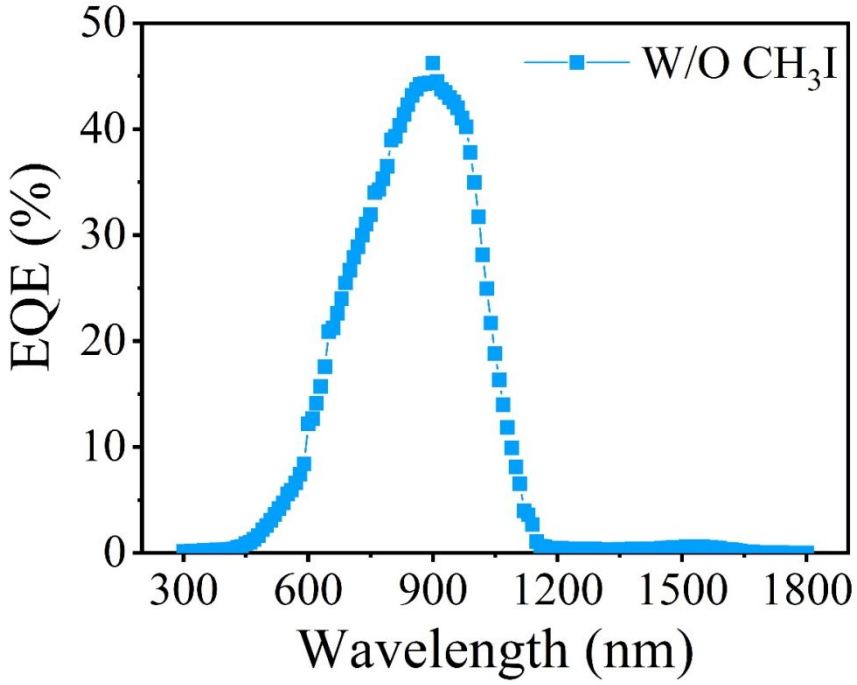

Figure S5. EQE of Si/PbS PD produced by the Si wafer without CH_3I passivation. It shows high EQE at the range below 1100 nm but quit low EQE at the range beyond 1100 nm, which indicating the charge transfer from PbS-EDT layer to Si wafer is inefficient without CH_3I passivation.

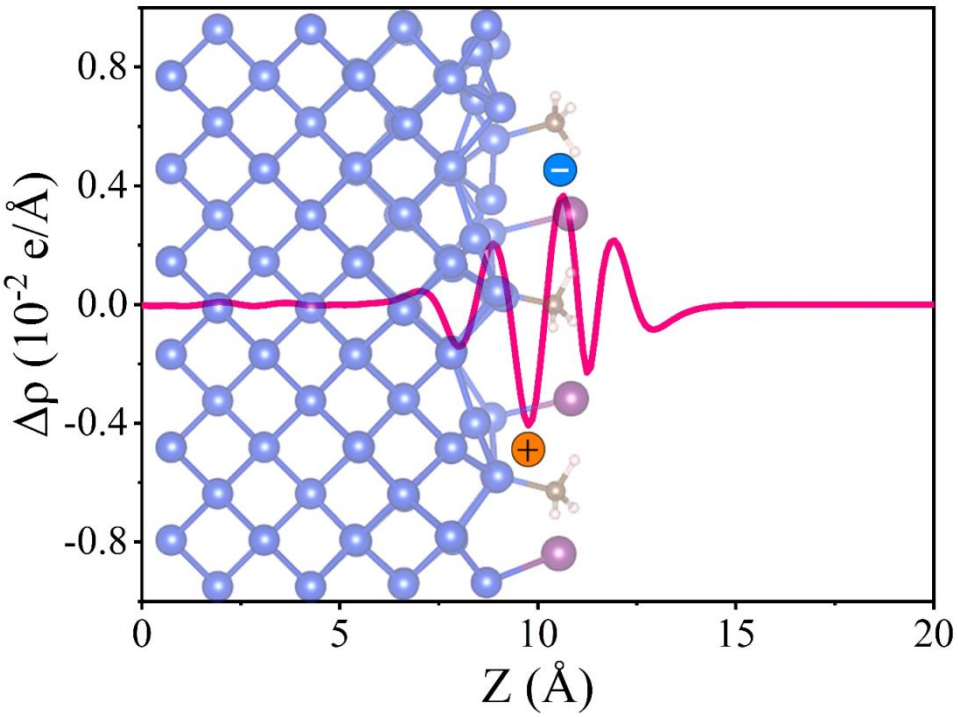

Figure S6. Charge density plot of the surface of Si wafer with CH_3I passivation calculated by density functional theory (DFT). The below layer is the illustration of methyl and iodine adsorption on Si surface, where the blue, purple and brown spheres represent the Si, I and C atoms respectively. Horizontal distance of the illustration corresponds to the plot's horizontal axis. The plot shows that the Si atoms on the surface have positive charges and the adsorbed methyl and iodine have negative charges, indicating the formation of negative surface dipole on Si surface with CH_3I passivation.

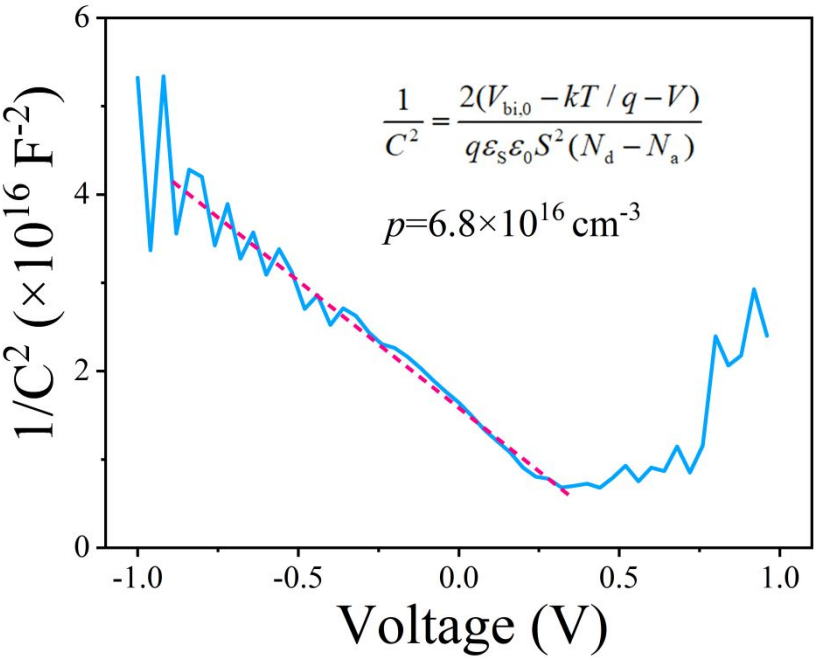

Figure S7. Capacitance voltage measurement of PbS-EDT layer. The doping density of PbS-EDT in this work was 6.8×10^{16} cm^{-3}

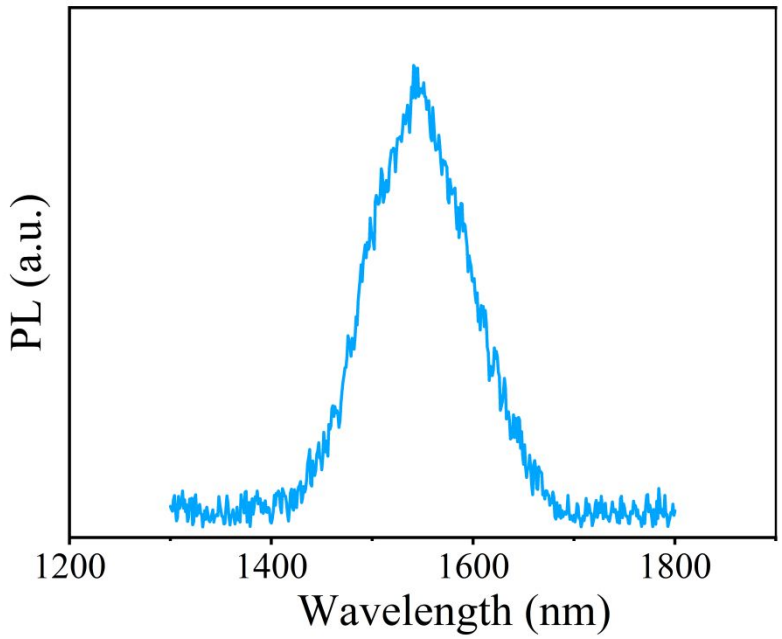

Figure S8. PL spectrum of PbS CQDs. The peak of it is about 1540 nm, 20 nm red-shift comparing with absorption spectrum.

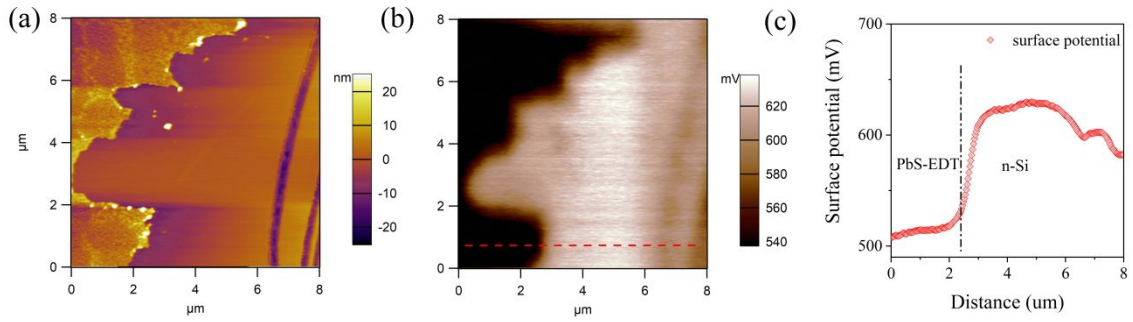

Figure S9. Atomic force microscope (AFM) and Kelvin probe force microscope (KPFM) characterization of Si/PbS-EDT sample. Silicon (CH_3I passivated) was partially covered with a thin PbS-EDT layer and the probe scanned vertically the step. (a) AFM mormology image and (b) surface potential distribution of Si/PbS-EDT sample. (c) Surface potential vs distance plot of the red line in (b).

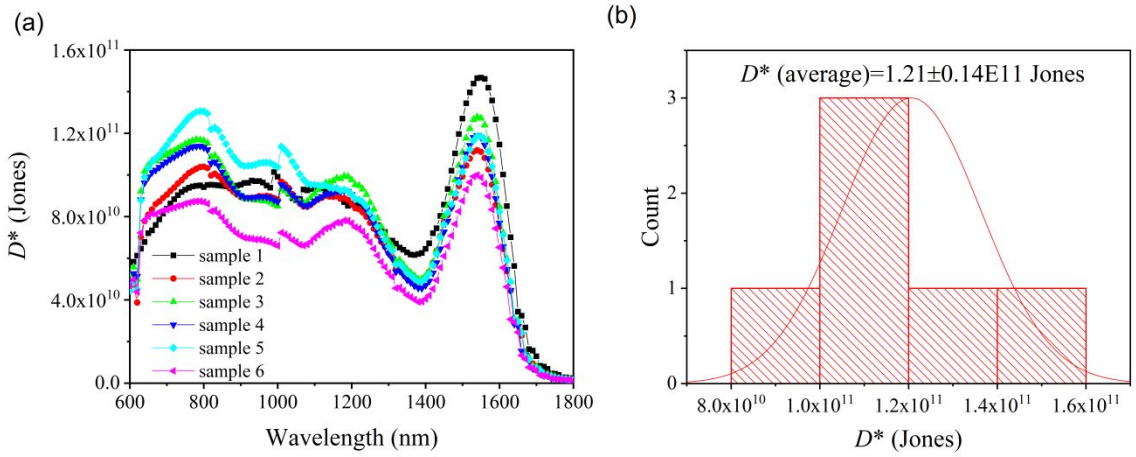

Figure S10. Detectivity statistics of inverted Si/PbS photodetectors. (a) Detectivity vs wavelength plots. (b) Detectivity distribution of the Si/PbS photodetectors. The average detectivity is 1.21E11 Jones and the standard deviation of is 0.14E11 Jones.

SCAPS modeling

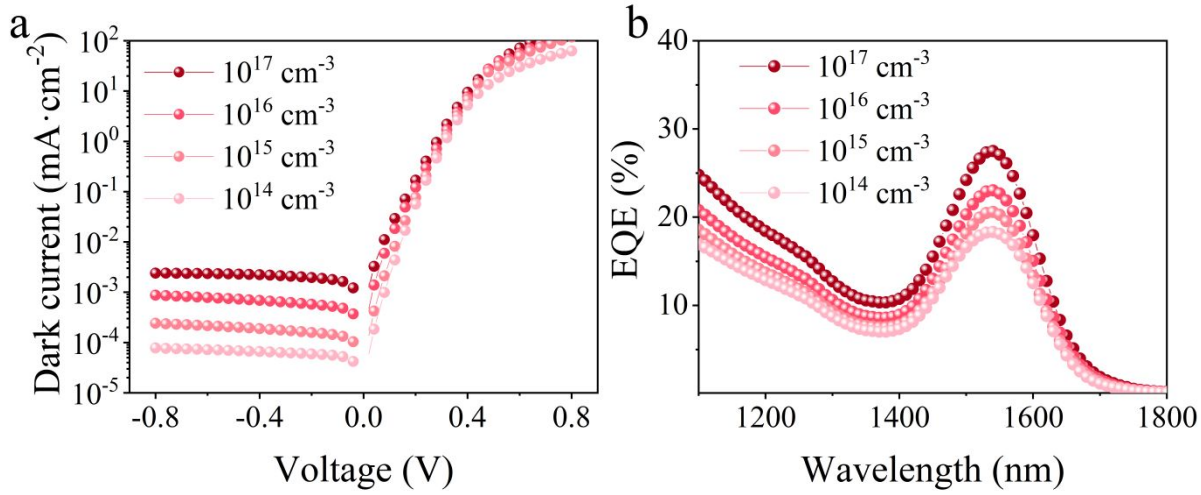

Figure S11. SCAPS simulative dark current (a) and EQE (b) of Si/PbS PD which produced by the Si wafers with different doping density. The results are consistent with the experimental results. The EQE and reverse dark current of them both increased as doping density increase.

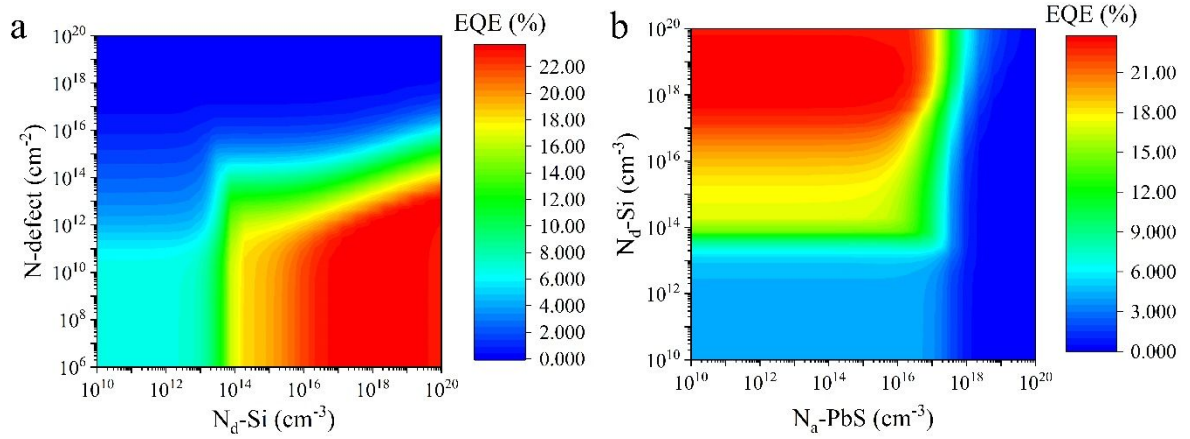

Figure S12. SCAPS simulation of inverted Si/PbS PD. (a) The simulated EQE for different doping density of n-Si wafer (N_d-Si) and surface defect density of n-Si wafer (N-defect). (b) The simulated EQE for different N_d-Si and the doping density of PbS layer (N_a-PbS). High N_d-Si, low N_a-PbS and low N-defect will result enhanced EQE.

Table S1. Physical parameters of the photodiode simulated using SCAPS software.

	PbS (EDT)	PbS (I)	n-Si(100)
bandgap (eV)	0.78	0.78	1.12
electron affinity (eV)	4.10	4.14	4.05
dielectric permittivity (relative)	20	20	11.8
CB effective density of states (1/cm^3)	1E19	1E19	2.82E19
VB effective density of states (1/cm^3)	1E19	1E19	1.83E19
electron thermal velocity (cm/s)	7E3	7E3	2.3E5
hole thermal velocity (cm/s)	7E3	7E3	1.5E5
electron mobility (cm^2/Vs)	5.5E-3	5.5E-3	1.4E3
hole mobility (cm^2/Vs)	5.5E-3	5.5E-3	4.5E2
shallow uniform donor density ND (1/cm3)	0	1E16	1.53E15
shallow uniform acceptor density NA (1/cm3)	6.8E16	0	0